



Thermal Transport Anomaly Associated with Weak Ferromagnetism in CaMnO_3

Hiroyuki FUJISHIRO, Shuichi OHSHIDEN and Manabu IKEBE

Faculty of Engineering, Iwate University, Morioka 020-8551

(Received December 9, 1999)

The thermal conductivity $\kappa(T)$, thermal diffusivity $\alpha(T)$ and magnetization $M(T)$ have been measured for sintered CaMnO_3 and $\text{La}_{1-x}\text{Ca}_x\text{MnO}_3$ in lightly electron-doped region ($0.98 \leq x \leq 1.0$). $\kappa(T)$ and $\alpha(T)$ of CaMnO_3 show an anomalous enhancement below the weak ferromagnetic transition temperature T_N . The enhancement is rapidly reduced by introduction of a small amount of Mn^{3+} ions in $\text{La}_{1-x}\text{Ca}_x\text{MnO}_3$. The analyses suggest the possibility that the enhancement comes from the contribution of the heat transport by magnetic excitations.

KEYWORDS: CaMnO_3 , thermal conductivity, thermal diffusivity, weak ferromagnetism, magnetic heat transport

§1. Introduction

Charge carrier doping into antiferromagnetic insulators with perovskite-related structures provides a stage where a variety of attractive phenomena such as the high T_c superconductivity, anomalous metallic state, metal-insulator transition, stripe order etc. are played. The background of the drama is the strong correlation between doped carriers, which has become one of main themes of recent physical concern. Recently, physical properties of perovskite-type manganites $\text{RE}_{1-x}\text{AE}_x\text{MnO}_3$ (RE = trivalent rare-earth ion, AE = divalent alkaline-earth ion) have been widely investigated in the hole-doped region ($x < 0.5$). In the electron-doped region ($x \approx 1.0$), however, the detailed reports are rather scarce.¹⁻⁷⁾ Several Ca-based $\text{RE}_{1-x}\text{Ca}_x\text{MnO}_3$ compounds have been recently investigated for $x \approx 1.0$ ³⁻⁸⁾ and a canted spin structure associated with pretty large negative magnetoresistance (MR) has been observed for $x \approx 0.9$. In order to perform detailed investigation of the electron-doping, we must have detailed information about the starting material, CaMnO_3 .

In this paper, we investigate the thermal transport properties of CaMnO_3 and $\text{La}_{1-x}\text{Ca}_x\text{MnO}_3$ ($x \approx 1.0$) polycrystals and report an anomaly observed in CaMnO_3 associated with the weak ferromagnetic order. A slight change of the Mn valency from Mn^{4+} to Mn^{3+} caused by the difference of oxygen content and/or by the electron doping drastically alters the thermal transport properties of this system. The anomaly in CaMnO_3 is rather difficult to understand on the basis of the phonon only heat conduction and the heat transport due to the magnetic collective modes seems to become important below its magnetic ordering temperature T_N . The thermal transport due to magnetic modes has been only scarcely studied. Several recent reports,⁹⁻¹¹⁾ however, have clearly demonstrated the magnetic mode contribution to the heat conduction. Systematic investigations on the theme of magnetic heat conduction are definitely

necessary.

§2. Experimental

CaMnO_3 and $\text{La}_{1-x}\text{Ca}_x\text{MnO}_3$ ($x = 0.99, 0.98$) samples were prepared from stoichiometric mixtures of CaCO_3 , La_2O_3 and Mn_3O_4 raw powders. The mixtures were calcined at 1000°C for 24 h in air, pressed into pellets and then sintered at 1500°C for 8 h in air. The sintered CaMnO_3 was named as “as-sintered” CaMnO_3 sample. The sintered CaMnO_3 and $\text{La}_{1-x}\text{Ca}_x\text{MnO}_3$ samples were heat-treated at 1500°C for 24 h in flowing oxygen to improve the oxygen non-stoichiometry and we named these samples as “ O_2 -annealed” samples. All the samples were confirmed to be in a single phase at room temperature by means of X-ray diffraction. The density of each sample was about 85% of the ideal one. The thermal conductivity $\kappa(T)$ and thermal diffusivity $\alpha(T)$ were automatically measured in a Gifford-McMahon cycle helium refrigerator as described elsewhere.^{12,13)} The magnetization M was measured by a SQUID magnetometer under a magnetic field of 0.5 T after zero field cooling. The thermal dilatation dL/L was measured by a strain gauge method.

§3. Results and Discussion

Figure 1 shows the temperature dependence of the thermal conductivity $\kappa(T)$ of O_2 -annealed CaMnO_3 , as-sintered CaMnO_3 and O_2 -annealed $\text{La}_{1-x}\text{Ca}_x\text{MnO}_3$ ($x = 0.99, 0.98$) samples. With decreasing temperature, $\kappa(T)$ of O_2 -annealed CaMnO_3 gradually decreases down to $T_m \approx 130$ K and then rapidly increases below T_m , showing a shallow minimum at T_m . With further decrease of T , $\kappa(T)$ takes a sharp maximum at $T_m \approx 40$ K, and then very steeply decreases. The as-sintered CaMnO_3 sample also shows similar $\kappa(T)$ behaviors, but the $\kappa(T)$ enhancement becomes moderate. In contrast, the maximum and the minimum of $\kappa(T)$ are almost wiped out for the O_2 -annealed $\text{La}_{1-x}\text{Ca}_x\text{MnO}_3$ samples; $\kappa(T)$ of $\text{La}_{0.02}\text{Ca}_{0.98}\text{MnO}_3$ shows a monotonic decrease with decreasing temperature, though some remnant of

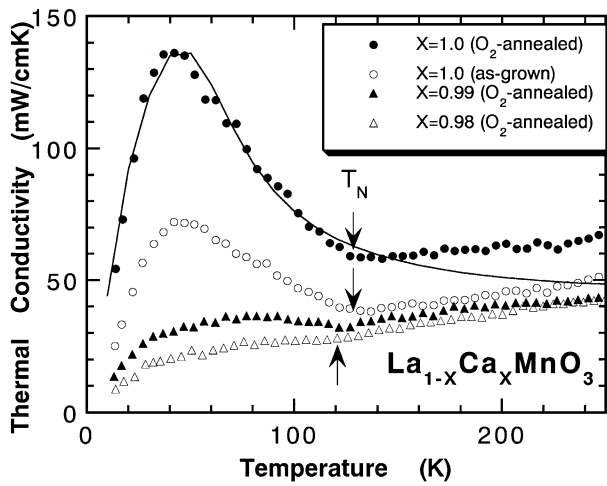


Fig. 1. Temperature dependence of the thermal conductivity $\kappa(T)$ of the CaMnO_3 (O_2 -annealed and as-sintered) and $\text{La}_{1-x}\text{Ca}_x\text{MnO}_3$ ($x = 0.99, 0.98$: O_2 -annealed) samples. The solid line shows the phonon conductivity κ_{ph} of O_2 -annealed CaMnO_3 calculated on the basis of eqs. (1) and (2). The fitting parameters are given in Table I. Note the discrepancy between the data and the calculated line for $T > T_N$.

the κ enhancement is noticeable for $\text{La}_{0.01}\text{Ca}_{0.99}\text{MnO}_3$ below $T \sim 120$ K.

Figure 2 presents the temperature dependence of the magnetization $M(T)$ under an applied field of 0.5 T. The $M(T)$ curves of the as-sintered and O_2 -annealed CaMnO_3 samples show a sharp increase at $T_N = 130$ K, which suggests the onset of the weak ferromagnetism (WF).¹⁴⁾ The magnitude of the WF moment is about $1/80$ of the Mn^{4+} moment ($\approx 3\mu_B$) and is slightly decreased by the O_2 annealing. What is to be noticed is that the $\kappa(T)$ minimum temperature T_m agrees with the WF ordering temperature T_N of the CaMnO_3 samples. The WF moment is slightly enhanced and T_N slightly decreases to 120 K by the 2% introduction of Mn^{3+} ions in $\text{La}_{0.02}\text{Ca}_{0.98}\text{MnO}_3$.

Figure 3 displays the thermal dilatation dL/L as a function of T . For all the samples, the contraction is somewhat enhanced at T_N with decreasing temperature. The slight enhancement in the gradient of dL/L at around T_N may suggest a possibility of a slight lattice change associated with the onset of the magnetic order. In Fig. 3, it is noteworthy that the anomalies of dL/L are almost of the same magnitude for the present samples, making a marked contrast to the different κ behavior in Fig. 1.

Figure 4 shows the electrical resistivity $\rho(T)$ of these samples. $\rho(T)$ is pretty large, behaves semiconductive and shows no anomaly at around T_N . From the Wiedemann-Franz law, the electrical contribution κ_e to the thermal conductivity is estimated to be negligibly small in these specimens. Then, in a usual sense, the heat conduction is overwhelmingly due to phonons. The phonon thermal conductivity κ_{ph} can be analyzed on the basis of the following relaxation time approximation.¹⁵⁾

$$\kappa_{\text{ph}} = \frac{3dnR}{2\pi M} \nu_s^2 \left(\frac{T}{\Theta_D} \right)^3 \int_0^{\Theta_D/T} \frac{x^4 e^x}{(e^x - 1)^2} \tau_{\text{ph}} dx, \quad (1)$$

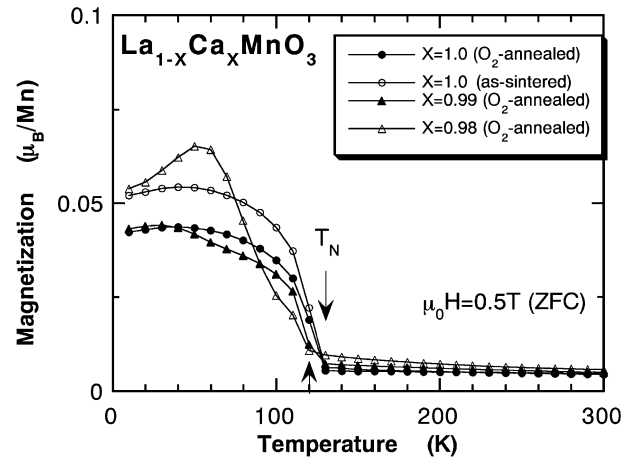


Fig. 2. Temperature dependence of the magnetization $M(T)$ of the CaMnO_3 and $\text{La}_{1-x}\text{Ca}_x\text{MnO}_3$ samples under an applied field of 0.5 T. The $M(T)$ curve of the CaMnO_3 samples shows a sharp increase at $T_N = 130$ K, which corresponds to the weak ferromagnetism onset.

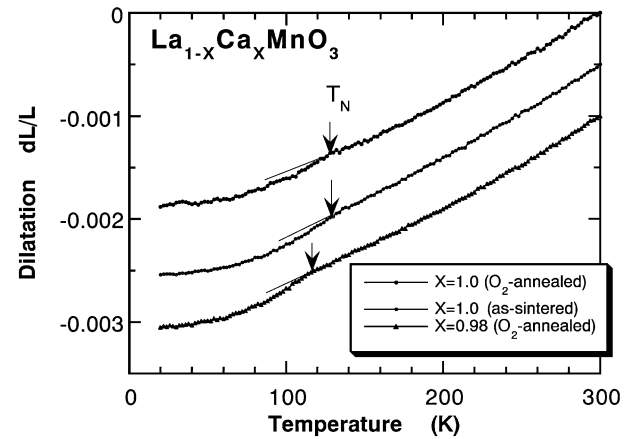


Fig. 3. The thermal dilatation dL/L as a function of T . The contraction of the samples with decreasing temperature is slightly enhanced at T_N in all samples.

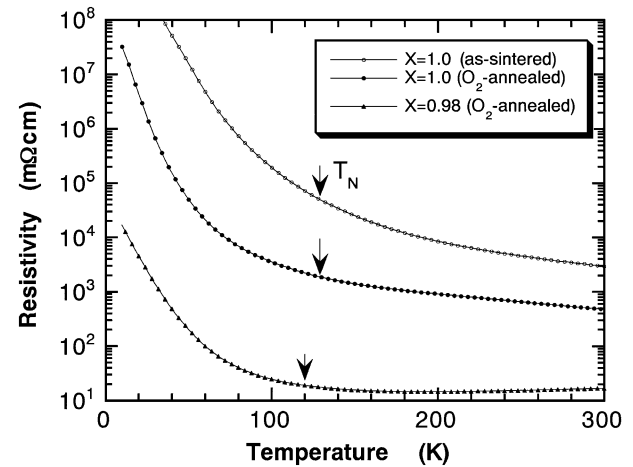


Fig. 4. Temperature dependence of the electrical resistivity of the CaMnO_3 (O_2 -annealed and as-sintered) and $\text{La}_{0.02}\text{Ca}_{0.98}\text{MnO}_3$ (O_2 -annealed) samples.

Table I. Summary of the parameters determined in the κ_{ph} fitting processes in $\text{La}_{1-x}\text{Ca}_x\text{MnO}_3$ samples on the basis of eqs. (1) and (2). The first three lines show the fitting parameters for the solid curves shown in Fig. 6. The last line shows the parameters for the solid curve shown in Fig. 1 in which the U term becomes dominant.

Sample	τ_{b}^{-1} (s^{-1})	l_{b} (μm)	s ($\text{K}^{-2}\text{s}^{-1}$)	p ($\text{K}^{-4}\text{s}^{-1}$)	U (s^{-1})
$X = 1.0$ (O_2 -annealed)	2.6×10^8	13.3	2.7×10^7	2.5×10^2	0
$X = 1.0$ (as-sintered)	2.6×10^8	13.3	4.2×10^7	3.9×10^2	0
$X = 0.98$ (O_2 -annealed)	7.2×10^8	4.9	6.1×10^7	3.6×10^2	0
$X = 1.0$ (O_2 -annealed)	2.9×10^8	13.3	2.2×10^5	2.1×10^3	7.1×10^{11}

where d is the mass density, n ($=5$ for $\text{La}_{1-x}\text{Ca}_x\text{MnO}_3$) the number of atoms in the chemical formula, M the molar weight, R the gas constant, ν_{s} the sound velocity, Θ_{D} the Debye temperature ($=400$ K) and x is the phonon frequency reduced by T . The phonon relaxation time is given by

$$\tau_{\text{ph}}^{-1} = \tau_{\text{b}}^{-1} + sT^2x^2 + pT^4x^4 + Ux \exp\left(-\frac{\Theta_{\text{D}}}{bT}\right). \quad (2)$$

Here, τ_{b}^{-1} refers to the phonon scattering strength by grain boundaries, s by the sheet-like defects and p by the point like defects. The last term with constant b (usually ≈ 2) stands for the phonon-phonon umklapp (U) processes.

What is the most puzzling for the heat conduction in the present samples is the $\kappa(T)$ minimum at around T_{N} of the CaMnO_3 samples. According to the analyses based on eqs. (1) and (2), the maximum at $T \approx 40$ K may be explained as to come from the U term, which becomes proceedingly dominant at higher temperatures. An example of $\kappa(T)$ fitting with parameter values in Table I are given by a solid line in Fig. 1 for O_2 -annealed CaMnO_3 . We had to adopt unusually small value $b = 1$ in the U term to get a remarkable fitting. As the fitting line demonstrates, κ_{ph} should continue to decrease with increasing temperature in the high temperature region because the U term with the exponential function has the strongest temperature dependence among the scattering terms in eq. (2). In case of very dirty crystals with strong phonon scattering by defects, however, the U term scattering can often actually be neglected because the phonon mean free path l_{ph} has been already strongly limited and almost saturated by defect scattering before the U processes limit l_{ph} .

Figure 5 shows the temperature dependence of the thermal diffusivity $\alpha(T)$ ($=\kappa/C = \nu_{\text{s}}l_{\text{ph}}/3$, if the heat conduction is purely of phonon origin, C : specific heat). Corresponding to the sharp increase of κ below T_{N} ($=T_{\text{m}}$), $\alpha(T)$ of O_2 -annealed and as-sintered CaMnO_3 abruptly increases below T_{N} with decreasing temperature. In contrast, $\alpha(T)$ of O_2 -annealed $\text{La}_{0.01}\text{Ca}_{0.99}\text{MnO}_3$ shows a moderate increase at lower temperatures. With increasing temperature above T_{N} , however, $\alpha(T)$ of all the samples shows a very slight decrease. Taking account of the measured ν_{s} value of $\nu_{\text{s}} \approx 7000$ m/s¹⁶) for $\text{La}_{1-x}\text{Ca}_x\text{MnO}_3$ ($x = 0.95$), the value of l_{ph} for O_2 -annealed CaMnO_3 is estimated to be ≈ 13 Å at T_{N} . This small value of l_{ph} suggests strong phonon scattering even in the O_2 -annealed CaMnO_3 sample. It is unreasonable that U processes abruptly become ineffective

for $T \geq T_{\text{N}}$, but the strength of the U process scattering should change continuously on temperature. The very steep change of $\alpha(T)$ of CaMnO_3 at T_{N} seems to suggest that some other heat conduction mechanism is operative for $T < T_{\text{N}}$. Because the $\alpha(T)$ and $\kappa(T)$ enhancement begins just at the magnetic order onset with decreasing T , the additional heat conduction mechanism should be related to collective magnetic excitations such as spin waves. Recently, the heat transport by magnetic excitations (κ_{spin}) was clearly demonstrated for CuGeO_3 ⁹) and for $\text{Sr}_{14-X}\text{A}_X\text{Cu}_{24}\text{O}_{41}$ ($\text{A}=\text{Ca}, \text{La}$).¹⁰) The possibility of heat conduction by spin waves was also suggested for non-superconductive $\text{YBa}_2\text{Cu}_3\text{O}_{6+\delta}$.¹¹) In the presence of κ_{spin} ($=C_{\text{spin}}\nu_{\text{spin}}l_{\text{spin}}/3$, C_{spin} : magnon specific heat, ν_{spin} : magnon velocity, l_{spin} : magnon mean free path), the diffusivity $\alpha = (\kappa_{\text{ph}} + \kappa_{\text{spin}})/C$ can abruptly increase below T_{N} .

In Fig. 6, we make a rough estimation of κ_{spin} by extrapolating κ_{ph} from $T > T_{\text{N}}$ on the basis of eqs. (1) and (2). The U term in eq. (2) is neglected assuming that the lattice defect scattering is strong enough. In this figure, the estimated κ_{ph} is presented by full lines. The used fitting parameters are summarized in Table I. The estimated contribution of magnons, $\kappa_{\text{spin}} = \kappa - \kappa_{\text{ph}}$, is presented by closed symbols for each sample. κ_{spin} of annealed and as-sintered CaMnO_3 is very large, while that of $\text{La}_{1-x}\text{Ca}_x\text{MnO}_3$ ($x = 0.99, 0.98$) is greatly diminished. The drastic reduction of κ_{spin} caused by a small amount of electron doping may probably be due to

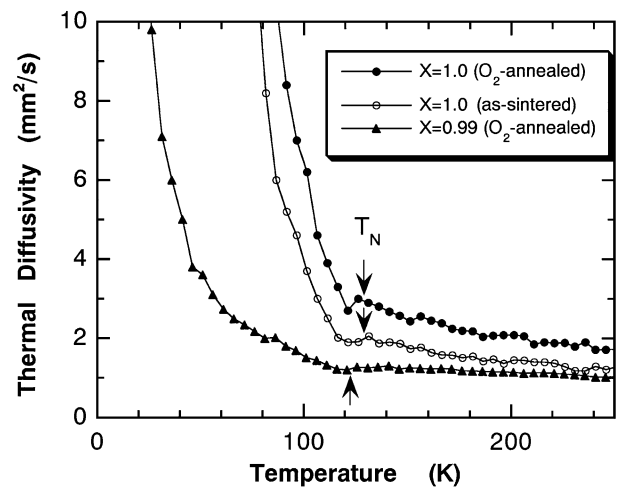


Fig. 5. The thermal diffusivity $\alpha(T)$ of the CaMnO_3 (O_2 -annealed and as-sintered) and $\text{La}_{0.01}\text{Ca}_{0.99}\text{MnO}_3$ (O_2 -annealed) samples as a function of T .

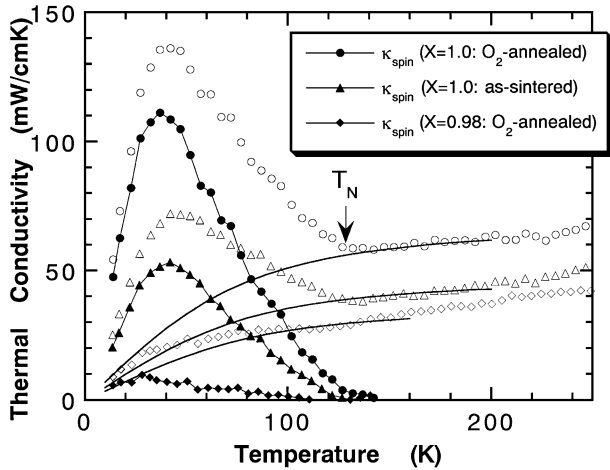


Fig. 6. The estimated phonon (κ_{ph}) and the magnetic (κ_{spin}) contributions to the thermal conductivity $\kappa(T)$. The phonon contribution κ_{ph} calculated on the basis of eqs. (1) and (2), and parameter values in Table I is presented by full lines. The contribution of the magnetic mode $\kappa_{\text{spin}} = \kappa - \kappa_{\text{ph}}$ is presented by closed symbols (see text).

magnon scattering by introduced Mn^{3+} impurity spins, which may strongly limit the magnon mean free path l_{spin} .

Assuming the magnon heat conduction, let us make a very rough estimation of the magnon mean free path l_{spin} of CaMnO_3 . We estimate the magnetic specific heat C_{spin} (erg/cm³) of Mn^{4+} spins based on the molecular field approximation and measured density d . The magnon velocity v_{spin} is estimated to be about 7.5×10^5 cm/s, assuming the antiferromagnetic dispersion (neglecting the weak ferromagnetic component),

$$\omega = v_{\text{spin}}q \approx \frac{2z|J|Saq}{\hbar}, \quad (3)$$

where, J is the exchange constant, z is the number of the nearest Mn spins, S ($=3/2$) is the spin quantum number of Mn^{4+} and a ($\approx 4 \text{ \AA}$) is the average distance between Mn ions. The exchange constant J is estimated from T_N again by use of the molecular field approximation,

$$T_N = \frac{2zJS(S+1)}{3k_B}, \quad (4)$$

where k_B is the Boltzmann constant. Based on these approximations, the maximum κ_{spin} ($T \approx 40 \text{ K}$) $\approx 110 \text{ mW/cmK}$ in Fig. 6 results in $l_{\text{spin}} \approx 800 \text{ \AA}$ or ~ 200 Mn atomic spacings. By doping 1% Mn^{3+} in $\text{La}_{0.01}\text{Ca}_{0.99}\text{MnO}_3$, the average Mn^{3+} distance is about 36 \AA or ~ 9 Mn spacings. The magnon mean free path can be reduced roughly to this value of the average Mn^{3+} distance as a result of Mn^{3+} impurity scattering and it is reasonable that 1% Mn^{3+} doping has drastically depressed the magnon heat conduction κ_{spin} .

Although we have emphasized the possibility of the magnon heat conduction, another possibility for the enhancement of $\kappa(T)$ and $\alpha(T)$ may be of phonon conduction origin. If we assume that Mn magnetic moment fluctuations strongly scatter phonons above T_N and that the phonon scattering by Mn spins is greatly reduced below

T_N in the magnetically ordered state, then the phonon thermal conduction is enhanced below T_N . Because spin fluctuations which we assume to scatter phonons must be reduced at low temperatures in the magnetically ordered state, this scenario provides a reasonable explanation for the $\kappa(T)$ behavior of CaMnO_3 . However, the drastic reduction of $\kappa(T)$ resulting from only 1% La substitution for Ca may be difficult to explain by this model; it seems unlikely that addition of only 1% Mn^{3+} spins so drastically enhances the spin fluctuations at low temperatures in the ordered state. It should be noticed again that the thermal dilatation dL/L in Fig. 3 shows almost the same behavior for CaMnO_3 and $\text{La}_{1-x}\text{Ca}_x\text{MnO}_3$ and there should be no significant lattice state difference in these samples between $T < T_N$ and $T > T_N$. The sound velocity measurement for $\text{La}_{0.05}\text{Ca}_{0.95}\text{MnO}_3$ showed quite a small change at T_N ,¹⁶⁾ supporting our conclusion from dL/L data.

§4. Summary

- i) The thermal conductivity $\kappa(T)$ and the thermal diffusivity $\alpha(T)$ were measured for CaMnO_3 and lightly electron-doped $\text{La}_{1-x}\text{Ca}_x\text{MnO}_3$ ($x \geq 0.98$) polycrystals. $\kappa(T)$ of CaMnO_3 gradually decreased with decreasing temperature down to the weak-ferromagnetic transition temperature T_N ($=120 \text{ K}$). Both $\kappa(T)$ and $\alpha(T)$ showed a peculiar enhancement with further reduction of temperature below T_N . Thus $\kappa(T)$ resulted in an unusual minimum at T_N . The $\kappa(T)$ and $\alpha(T)$ enhancement below T_N was very rapidly suppressed by introduction of Mn^{3+} spins in $\text{La}_{1-x}\text{Ca}_x\text{MnO}_3$.
- ii) The thermal dilatation dL/L showed a small anomaly at T_N and the behaviors of dL/L were very similar for CaMnO_3 and $\text{La}_{1-x}\text{Ca}_x\text{MnO}_3$. The difference of $\kappa(T)$ and $\alpha(T)$ behaviors between CaMnO_3 and $\text{La}_{1-x}\text{Ca}_x\text{MnO}_3$ cannot be explained as coming from the difference in the lattice states.
- iii) The thermal diffusivity remained almost constant above T_N and the phonon mean free path l_{ph} ($T \approx T_N$) estimated from the $\alpha(T)$ values was as small as $\approx 13 \text{ \AA}$ for O_2 -annealed CaMnO_3 . This fact implies that a strong phonon scattering mechanism which almost saturates l_{ph} is at work at least for $T > T_N$ even in this best heat conducting sample.
- iv) As possible origins of the heat transport enhancement below T_N , two possibilities were discussed. One is the magnon heat conduction κ_{spin} which may be operative below T_N . The other is the phonon conduction strongly limited by the scattering by spin fluctuations. Although the effect of electron (Mn^{3+}) doping seems to strongly suggest the importance of κ_{spin} , we cannot arrive at an unambiguous answer at the present stage. The thermal transport measurements in very strong magnetic fields may provide an important clue to distinguish the two scenarios.

Acknowledgment

The authors wish to thank T. Kikuchi of Iwate University for his assistance in sample fabrication and Prof. T. Fukase of Tohoku University for the collaboration in

the sound velocity measurements. The present study is partially supported by REIMEI Research Resources of Japan Atomic Energy Research Institute.

-
- 1) E. O. Wollan and W. C. Koehler: *Phys. Rev.* **100** (1955) 545.
 - 2) Z. Jirak, S. Krupicka, Z. Simsa, M. Dlouha and S. Vratislav: *J. Magn. Magn. Mater.* **53** (1985) 153.
 - 3) H. Chiba, M. Kikuchi, K. Kusaba, Y. Muraoka and Y. Shono: *Solid State Commun.* **99** (1996) 499.
 - 4) Wei Bao, J. D. Axe, C. H. Chen and S-W. Cheong: *Phys. Rev. Lett.* **78** (1997) 543.
 - 5) I. O. Troyanchuk, N. V. Samsonenko, H. Szymczak and A. Nabialek: *J. Solid State Chem.* **131** (1997) 144.
 - 6) C. Martin, A. Maignan, F. Damay and B. Raveau: *J. Solid State Chem.* **134** (1997) 198.
 - 7) A. Maignan, C. Martin, F. Damay, B. Reveau and J. Hejtmanek: *Phys. Rev. B* **58** (1998) 2758.
 - 8) H. Fujishiro, M. Ikebe, S. Ohshiden and K. Noto: *J. Phys. Soc. Jpn.* **69** (2000) 1865.
 - 9) Y. Ando, J. Takenaka, D. L. Sisson, S. G. Doettinger, I. Tanaka, R. S. Feigelson and A. Kapitulnik: *Phys. Rev. B* **58** (1998) R2913.
 - 10) K. Kudo, S. Ishikawa, T. Noji, T. Adachi, Y. Koike, K. Maki, S. Tsuji and K. Kumagai: *J. Low Temp. Phys.* **117** (1999) 1689.
 - 11) K. Takenaka, Y. Fukuzumi, K. Mizuhashi, S. Uchida, H. Asaoka and H. Takei: *Phys. Rev. B* **56** (1997) 5654.
 - 12) H. Fujishiro, T. Naito, M. Ikebe and K. Noto: *Cryogenic Engineering* **28** (1993) 533 [in Japanese].
 - 13) M. Ikebe, H. Fujishiro, T. Naito and K. Noto: *J. Phys. Soc. Jpn.* **63** (1994) 3107.
 - 14) J. B. MacCesney, H. J. Williams, J. F. Potter and R. C. Sherwood: *Phys. Rev.* **164** (1967) 779.
 - 15) R. Berman: *Thermal Conductivity in Solids* (Clarendon Press, Oxford, NewYork, 1976).
 - 16) T. Fukase: private communication.
-